

## SUPPORTING INFORMATION

### **Regulated Crystallization of Efficient and Stable Tin-based Perovskite Solar Cells via Self-sealing Polymer**

*Gengling Liu<sup>a,b</sup>, Cong Liu<sup>a,b</sup>, Zhuojia Lin<sup>a,b</sup>, Jia Yang<sup>a,b</sup>, Zengqi Huang<sup>a,b</sup>, Licheng Tan<sup>\*a,b</sup>, Yiwang Chen<sup>\*a,b,c</sup>*

G. Liu, C. Liu, Z. Lin, J. Yang, Z. Huang, Prof. Dr. L. Tan, Prof. Dr. Y. Chen

<sup>a</sup> College of Chemistry, Nanchang University, 999 Xuefu Avenue, Nanchang 330031, China.

<sup>b</sup> Institute of Polymers and Energy Chemistry (IPEC), Nanchang University, 999 Xuefu Avenue, Nanchang 330031, China.

<sup>c</sup> Institute of Advanced Scientific Research (iASR), Jiangxi Normal University, 99 Ziyang Avenue, Nanchang 330022, China.

\*Corresponding Authors: tanlicheng@ncu.edu.cn (L. Tan); ywchen@ncu.edu.cn (Y. Chen).

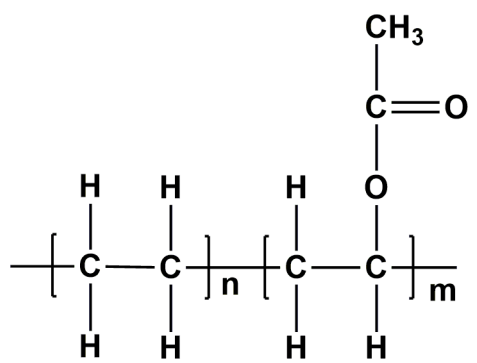


**Figure S1.** Molecular structure of EVA.

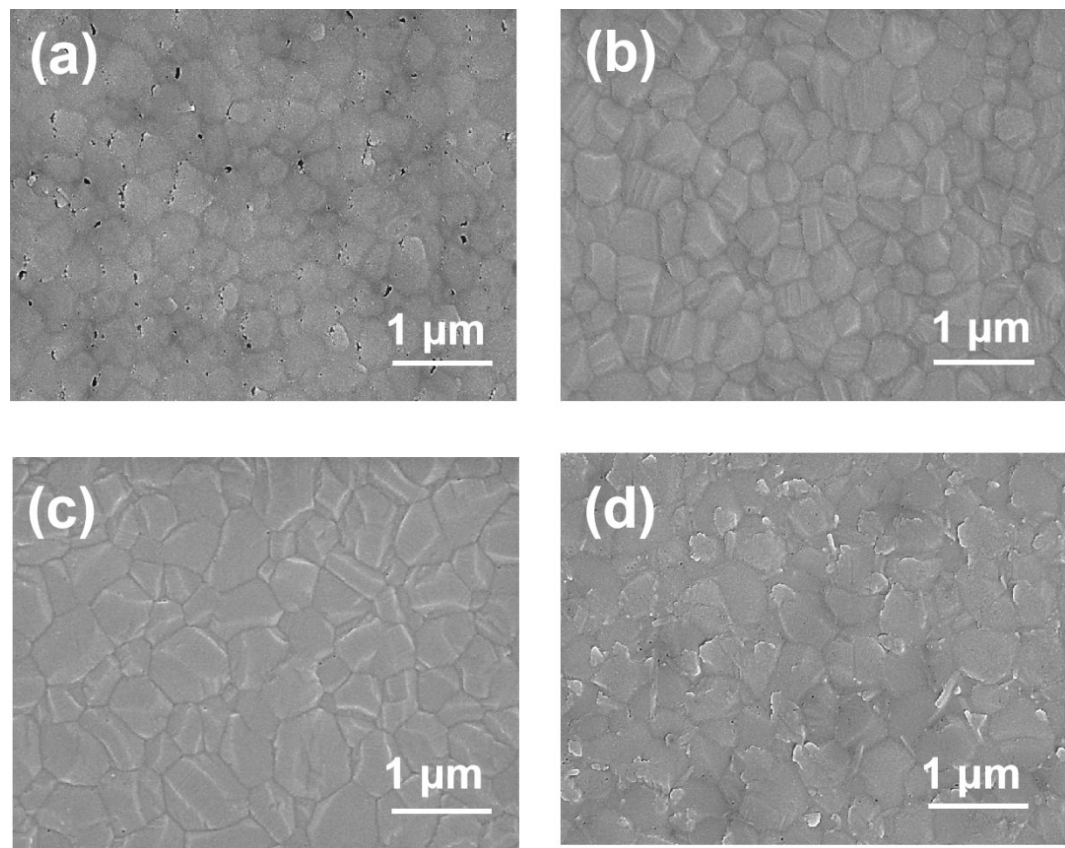


**Figure S2.** SEM images of perovskite films treated by EVA with different concentrations: (a) 0 mg/mL, (b) 1 mg/mL, (c) 2 mg/mL and (d) 5 mg/mL.

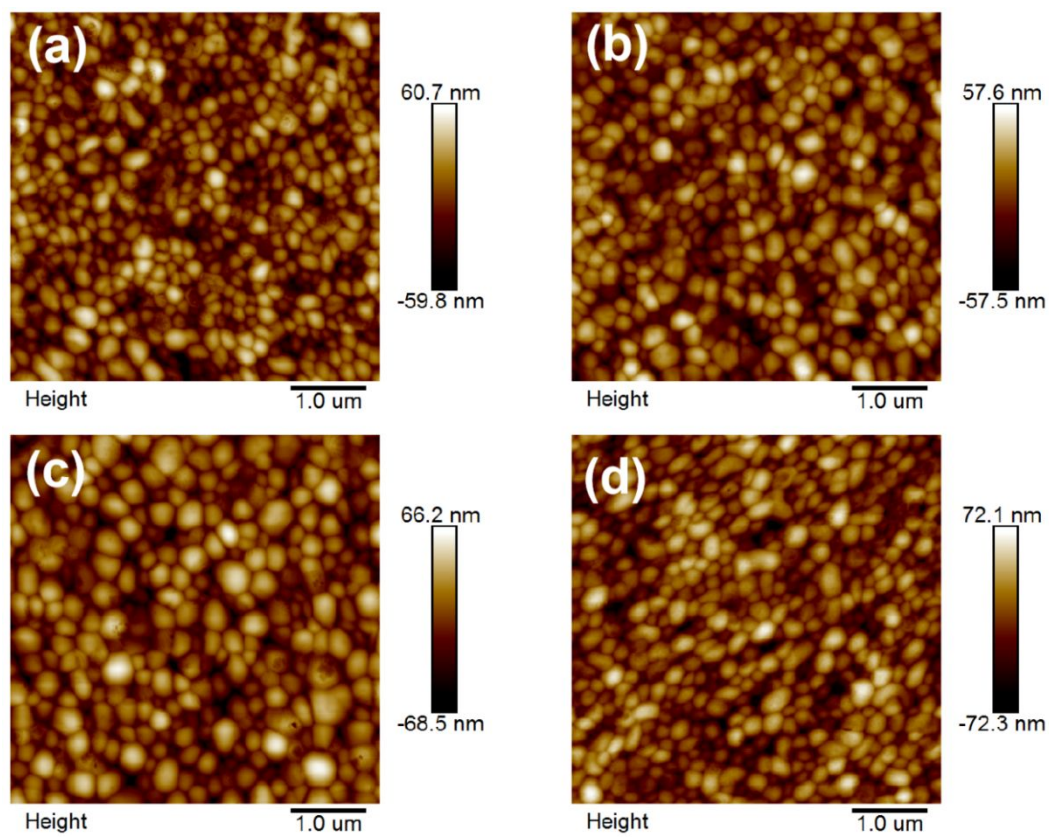


**Figure S3.** AFM height images of perovskite films treated by EVA with different concentrations: (a) 0 mg/mL, (b) 1 mg/mL, (c) 2 mg/mL and (d) 5 mg/mL.

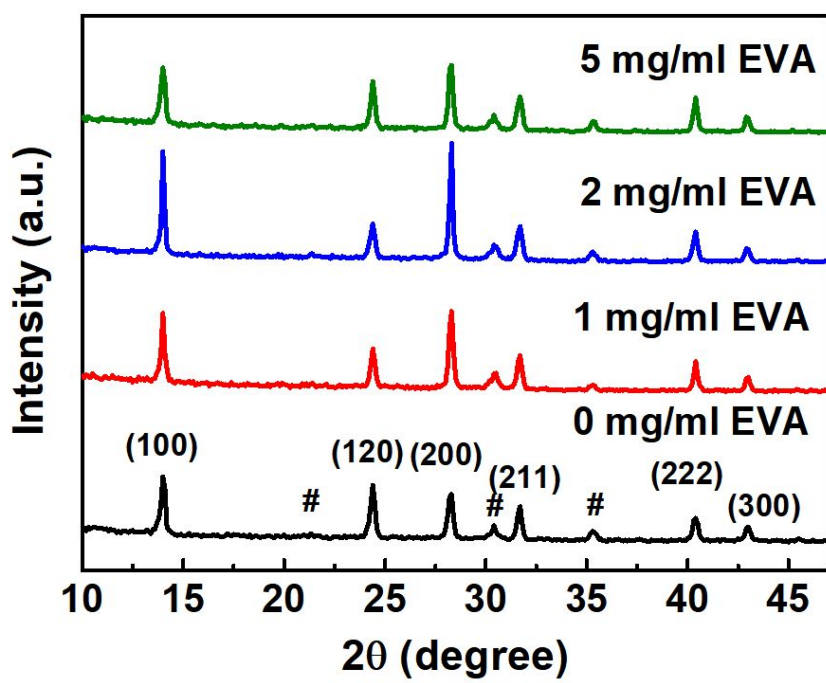


**Figure S4.** GIXRD patterns of perovskite films treated by EVA with different concentrations (0 mg/mL, 1 mg/mL, 2 mg/mL and 5 mg/mL).

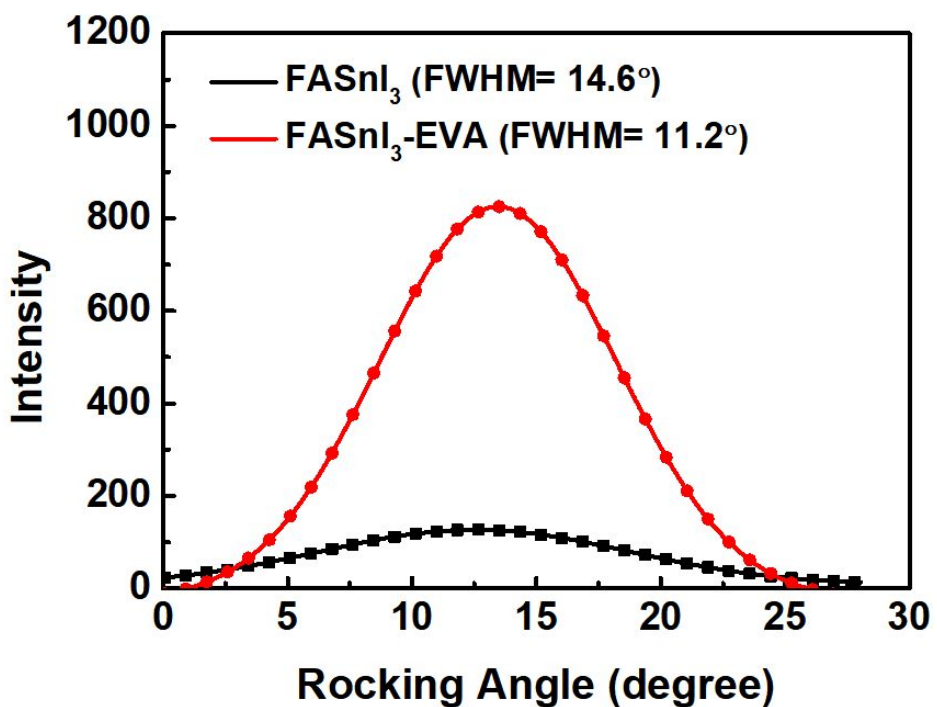


**Figure S5.** X-ray diffraction rocking curves of the (200) plane for the FASnI<sub>3</sub> and FASnI<sub>3</sub>-EVA perovskite films, respectively.

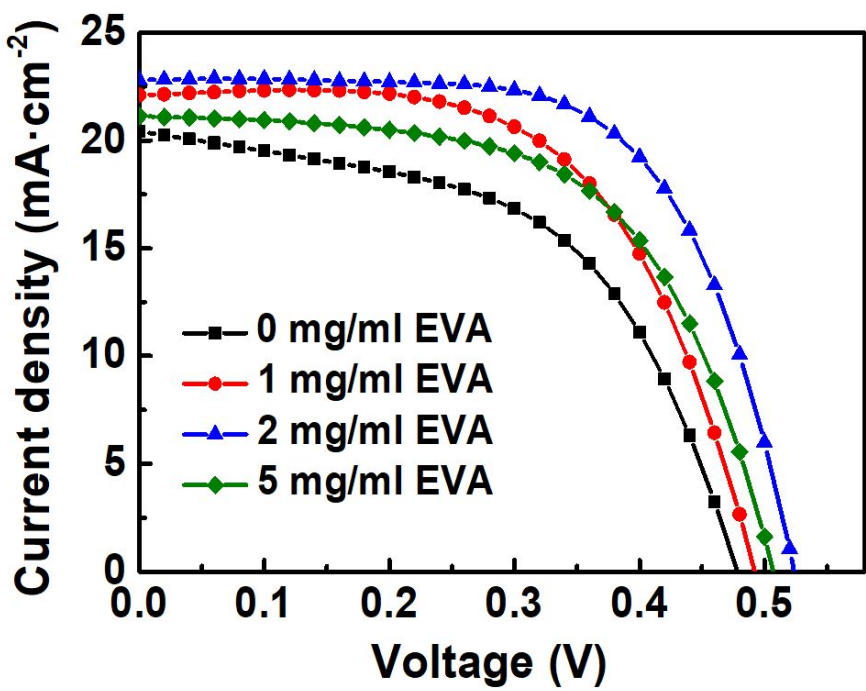


**Figure S6.** *J-V* curves of the PVSCs with different concentrations (0 mg/mL, 1 mg/mL, 2 mg/mL, 5 mg/mL) of EVA treatment.

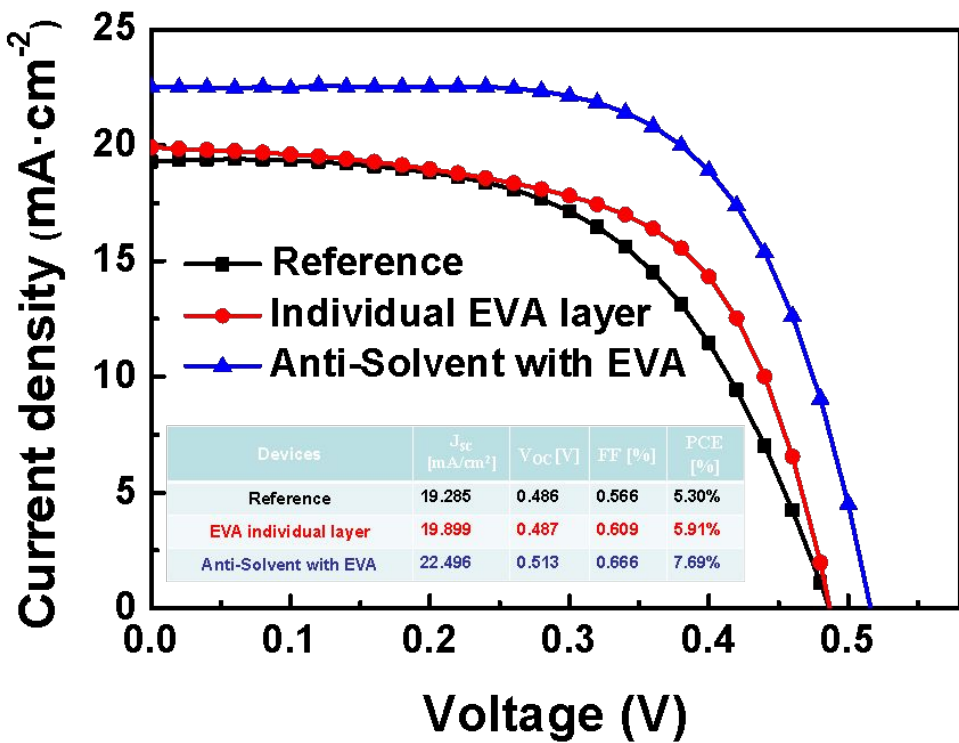


**Figure S7.**  $J-V$  curves of the PVSCs fabricated by conventional CB anti-solvent (reference), anti-solvent with EVA and spin-coating an individual EVA layer, respectively.

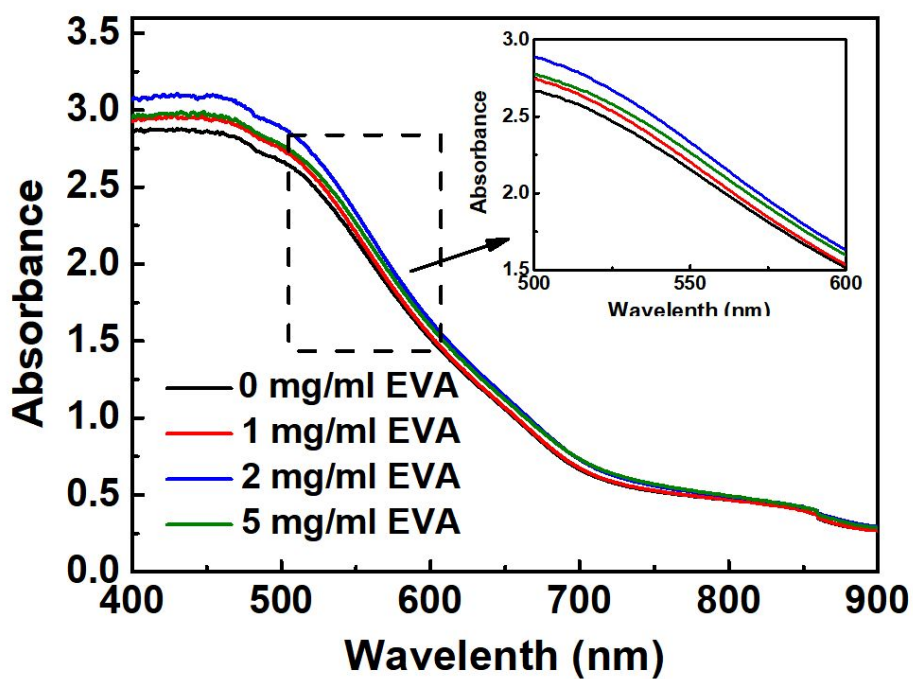


**Figure S8.** UV-vis absorption spectra of perovskite films that treated by EVA with different concentrations (0 mg/mL, 1 mg/mL, 2 mg/mL and 5 mg/mL).

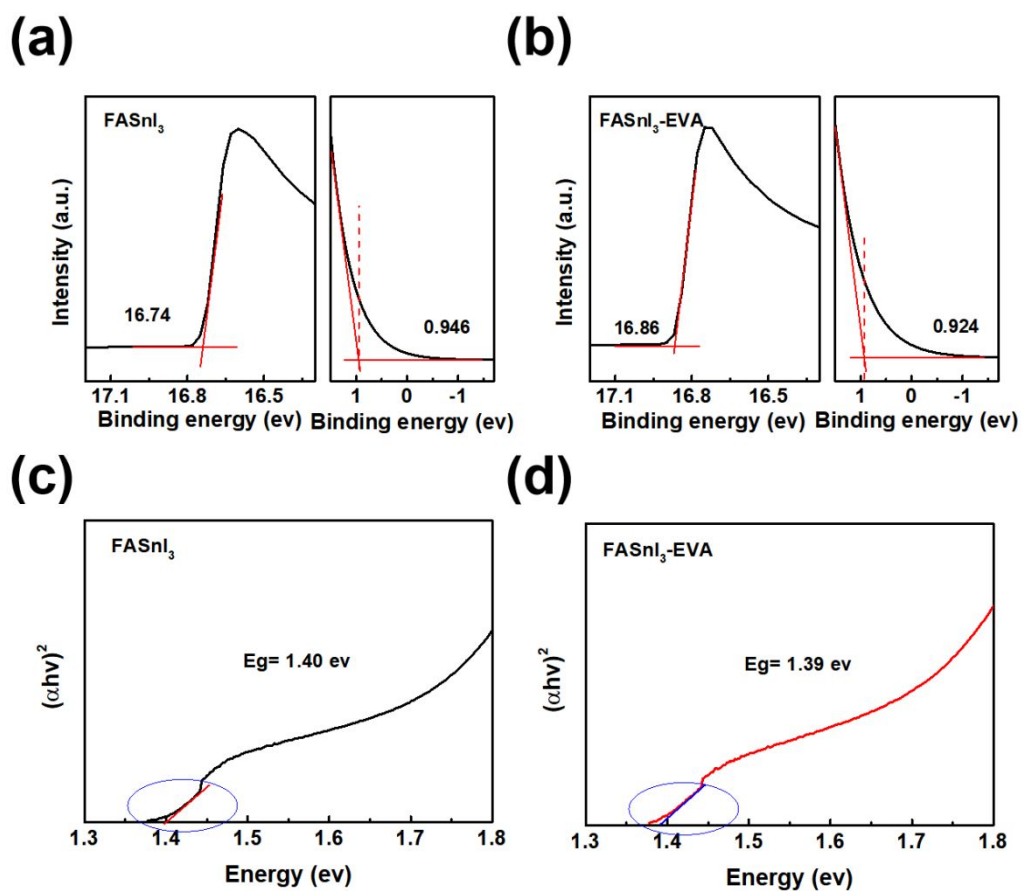


**Figure S9.** Ultraviolet photoelectron spectroscopy (UPS) of secondary electron cut off and valence band of the FASnI<sub>3</sub> films without (a) and with (b) EVA treatment. The relationship of  $(\alpha h\nu)^2$  vs energy for the FASnI<sub>3</sub> films without (c) and with (d) EVA treatment.

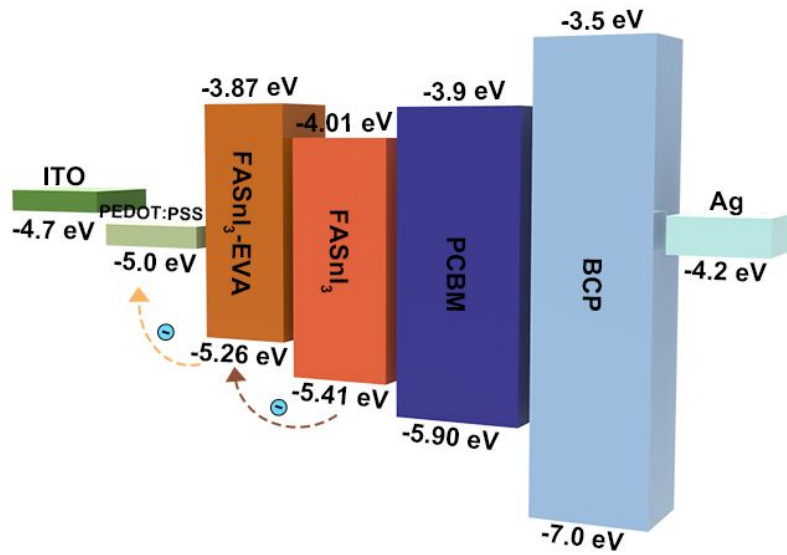


**Figure S10.** Schematic energy level diagram of materials used in the fabricated perovskite solar cells.

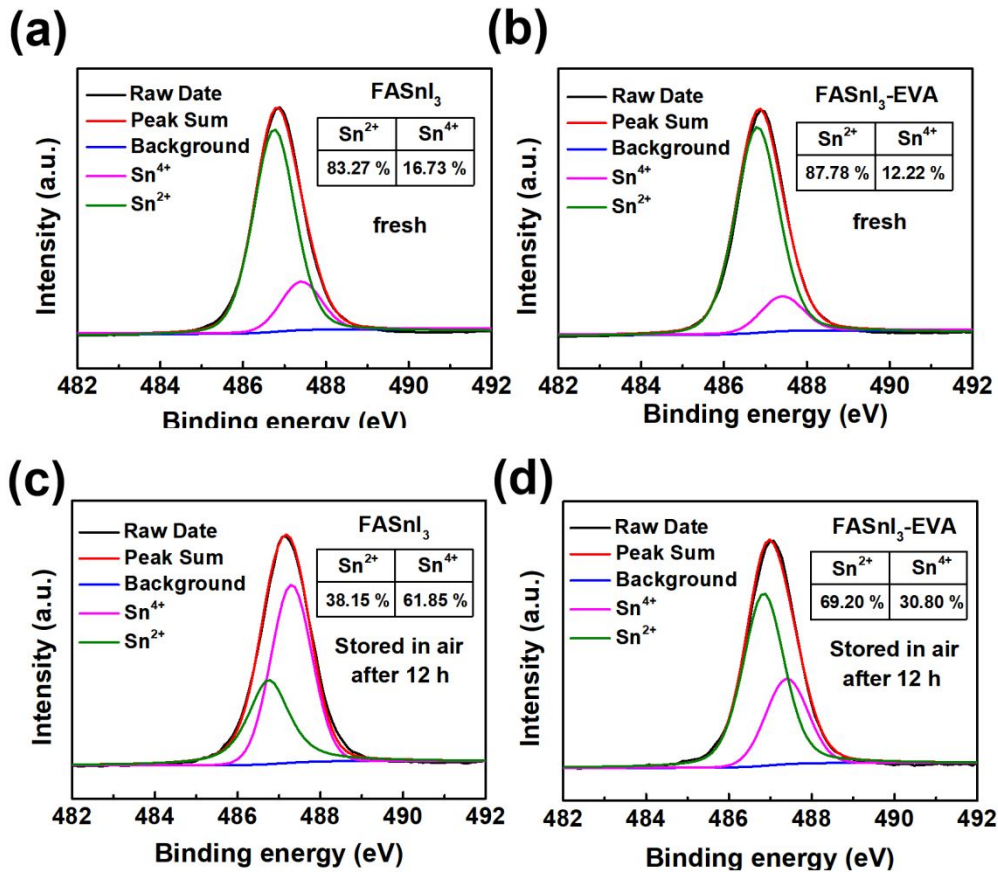


**Figure S11.** X-ray photoelectron spectra of the fresh FASnI<sub>3</sub> perovskite films without (a) or with (b) EVA treatment. X-ray photoelectron spectra of the ageing (stored in air for 12h) FASnI<sub>3</sub> perovskite films without (c) and with (d) EVA treatment

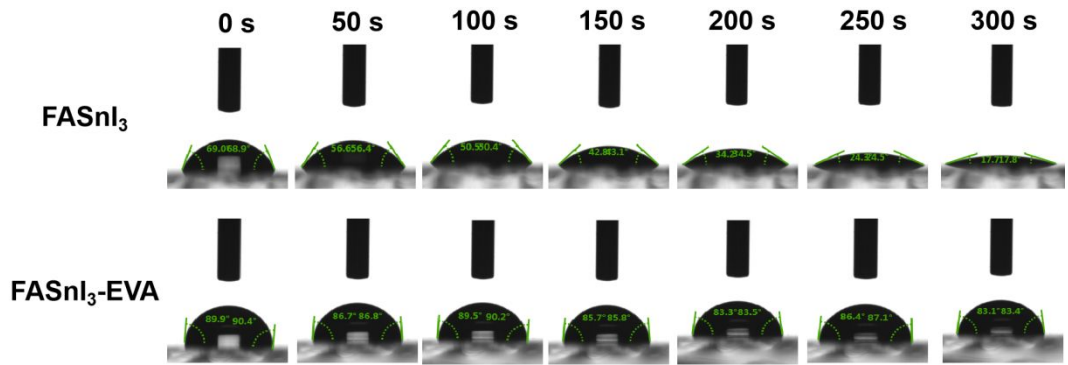


**Figure S12.** Contact angles of water droplets for FASnI<sub>3</sub> and FASnI<sub>3</sub>-EVA perovskite films under different recording times (0-300 s).

**Table S1.** The current density-voltage ( $J$ - $V$ ) parameters of the FASnI<sub>3</sub> based PVSCs treated by EVA with different concentrations (0 mg/mL, 1 mg/mL, 2 mg/mL and 5 mg/mL).

EVA concentration	$V_{oc}$ (V)	$J_{sc}$ (mA/cm <sup>2</sup> )	FF (%)	PCE (%)
0 mg/mL	0.487	20.433	53.474	5.23%
1 mg/mL	0.492	22.104	59.738	6.50%
2 mg/mL	0.523	22.800	64.690	7.72%
5 mg/mL	0.507	21.130	59.387	6.36%

**Table S2.** The parameters of time-resolved photoluminescence (TRPL) measurements for FASnI<sub>3</sub> films deposited on glass substrate without and with EVA treatment.

Sample	$\tau_1$ (ns)	Ratio (%)	$\tau_2$ (ns)	Ratio (%)	$\tau_{ave}$ (ns)
FASnI <sub>3</sub>	0.123	53.39	1.635	46.61	1.53
FASnI <sub>3</sub> -EV	0.135	41.40	3.063	58.60	2.97
A					

The average PL lifetime ( $\tau_{ave}$ ) values were obtained by the intensity average

method, given by  $\frac{\sum_{i=1}^n A_i \tau_i^2}{\sum_{i=1}^n A_i \tau_i}$ .

**Table S3.** The band structure parameters of the FASnI<sub>3</sub> film without and with EVA treatment.

Sample	E <sub>cutoff</sub> (eV)	E <sub>onset</sub> (eV)	HOMO (eV)	LUMO (eV)
FASnI <sub>3</sub>	16.74	0.946	-5.406	-4.006
FASnI <sub>3</sub> -EVA	16.86	0.924	-5.264	-3.874

The lowest unoccupied molecular orbital (LUMO) levels were calculated by the formula:  $E_{\text{LUMO}} = - [E_g + 21.22 - (E_{\text{cutoff}} - E_{\text{onset}})]$  eV. The optical bandgap was estimated from the onset position of the absorption spectra and calculated by the equation:  $E_g = 1240/\lambda_{\text{onset}}$ .

**Table S4.** The lifetimes of FASnI<sub>3</sub> based PVSCs stored in air without encapsulation.

Absorber	Structure	PCE	Storage environment	Lifetime (Keep the initial value)	Ref
FASnI <sub>3</sub> (SnCl <sub>2</sub> +KHQSA)	Inverted	6.67%	Air (RH=20%)	500 h ( $\approx 80\%$ )	[1]
			Air (RH=45%)	168 h ( $\approx 80\%$ )	
FASnI <sub>3</sub> (SnF <sub>2</sub> )	Inverted	5.12%	N <sub>2</sub> glove box	720 h ( $\approx 95\%$ )	[2]
			Air (RH=40%)	8 h ( $\approx 65\%$ )	
FASnI <sub>3</sub> (SnF <sub>2</sub> +PEAI)	Inverted	9.0%	Air (RH=20%)	80 h ( $\approx 60\%$ )	[2]
FASnI <sub>3</sub> (SnF <sub>2</sub> +TMA)	Inverted	7.09%	N <sub>2</sub> glove box	480 h ( $\approx 80\%$ )	[3]
			Air (RH=50%)	20 h (0%)	
Air					
FA <sub>0.75</sub> MA <sub>0.25</sub> SnI <sub>3</sub>	Inverted	3.31%	(Humidity unknown)	1 h (0%)	[4]
FASnI <sub>3</sub> (SnF <sub>2</sub> +5-AVAI)	Inverted	7.0%	N <sub>2</sub> glove box	1000 h ( $\approx 90\%$ )	[5]
			Air (RH=50%)	50 h ( $\approx 40\%$ )	
FASnI <sub>3</sub> (SnF <sub>2</sub> +PPAI)	Inverted	9.61%	N <sub>2</sub> glove box	1440 h ( $\approx 92\%$ )	[6]
			Air (RH=60%)	10 h ( $\approx 60\%$ )	
FASnI <sub>3</sub> (SnF <sub>2</sub> +EVA)	Inverted	7.72%	N <sub>2</sub> glove box	<b>800 h (90.1%)</b>	This work
			Air (RH=60%)	<b>48 h (62.4%)</b>	

## References

- [1]. Tai, Q.; Guo, X.; Tang, G.; You, P.; Ng, T. W.; Shen, D.; Cao, J.; Liu, C. K.; Wang, N.; Zhu, Y. Antioxidant Grain Passivation for Air-Stable Tin-Based Perovskite Solar Cells. *Angew. Chem. Int. Ed.* **2019**, 58, 806-810.
- [2]. Shao, S.; Liu, J.; Portale, G.; Fang, H. H.; Blake, G. R.; ten Brink, G. H.; Koster, L. J. A.; Loi, M. A. Highly Reproducible Sn-Based Hybrid Perovskite Solar Cells with 9% Efficiency. *Adv. Energy Mater.* **2018**, 8, 1702019.
- [3]. Zhu, Z.; Chueh, C. C.; Li, N.; Mao, C.; Jen, A. K. Y. Realizing Efficient Lead-Free Formamidinium Tin Triiodide Perovskite Solar Cells via a Sequential Deposition Route. *Adv. Mater.* **2018**, 30, 1703800.
- [4]. Ito, N.; Kamarudin, M. A.; Hirotani, D.; Zhang, Y.; Shen, Q.; Ogomi, Y.; Iikubo, S.; Minemoto, T.; Yoshino, K.; Hayase, S. Mixed Sn-Ge Perovskite for Enhanced Perovskite Solar Cell Performance in Air. *J. Phys. Chem. Lett.* **2018**, 9, 1682-1688.
- [5]. Kayesh, M. E.; Matsuishi, K.; Kaneko, R.; Kazaoui, S.; Lee, J. J.; Noda, T.; Islam, A. Coadditive Engineering with 5-Ammonium Valeric Acid Iodide for Efficient and Stable Sn Perovskite Solar Cells. *ACS Energy Lett.* **2019**, 4, 278-284.
- [6]. Ran, C.; Gao, W.; Li, J.; Xi, J.; Li, L.; Dai, J.; Yang, Y.; Gao, X.; Dong, H.; Jiao, B. Conjugated Organic Cations Enable Efficient Self-Healing FASnI<sub>3</sub> Solar Cells. *Joule* **2019**, 3, 3072-3087.